Chemical and Hydrostatic Pressure in Natrolites: Pressure-Induced Hydration of an Aluminogermanate Natrolite

ARTICLE *in* THE JOURNAL OF PHYSICAL CHEMISTRY C · OCTOBER 2010

Impact Factor: 4.77 · DOI: 10.1021/jp106964j

6 AUTHORS, INCLUDING:

Yongjae Lee
Yonsei University
168 PUBLICATIONS **2,461** CITATIONS
SEE PROFILE

Jianming Bai
Brookhaven National Laboratory
138 PUBLICATIONS **2,230** CITATIONS
SEE PROFILE

John B Parise
Stony Brook University
192 PUBLICATIONS **4,897** CITATIONS
SEE PROFILE

Thomas Vogt
University of South Carolina
360 PUBLICATIONS **9,225** CITATIONS
SEE PROFILE

Chemical and Hydrostatic Pressure in Natrolites: Pressure-Induced Hydration of an Aluminogermanate Natrolite

Yongjae Lee,[†] Dong-Hoon Seoung,[†] Jianming Bai,[‡] Chi-Chang Kao,[‡] John B. Parise,[§] and Thomas Vogt*,[||]

Department of Earth System Sciences, Yonsei University, Seoul 120-749, Korea, National Synchrotron Light Source, Brookhaven National Laboratory, Upton, New York 11973, Department of Geosciences, State University of New York, Stony Brook, New York 11794, and NanoCenter & Department of Chemistry and Biochemistry, University of South Carolina, Columbia, South Carolina 29208

Received: July 26, 2010; Revised Manuscript Received: September 24, 2010

The ambient structure and pressure-induced structural changes of a synthetic sodium aluminogermanate with a natrolite (NAT) framework topology (Na−AlGe-NAT) were characterized by using Rietveld refinements of high-resolution synchrotron X-ray powder diffraction data at ambient and high pressures. Unlike a previously established model for $Na_8Al_8Ge_{12}O_{40}\cdot 8H_2O$ based on a single-crystal study, the ambient structure of the Na−AlGe-NAT is found to adopt a monoclinic space group **C***c* (or **F***d*) with a ca. 6% expanded unit cell. The refined ambient structure of $Na_8Al_8Ge_{12}O_{40}\cdot 12H_2O$ indicates an increased water content of 50%, compared to the single-crystal structure. The unit-cell volume and water-content relationships observed between the two Na−AlGe-NAT structures at ambient conditions with 8 and 12 H_2O respectively seem to mirror the ones found under hydrostatic pressure between the $Na_8Al_8Si_{12}O_{40}\cdot 8H_2O$ and the parantrolite phase $Na_8Al_8Si_{12}O_{40}\cdot 12H_2O$. Under hydrostatic pressures mediated by a pore-penetrating alcohol and water mixture, the monoclinic Na−AlGe-NAT exhibits a gradual decrease of the unit-cell volume up to ca. 2.0 GPa, where the unit-cell volume then contracts abruptly by ca. 4.6%. This is in marked contrast to what is observed in the Na−AlSi-NAT and Na−GaSi-NAT systems, where one observes a pressure-induced hydration and volume expansion due to the auxetic nature of the frameworks. Above 2 GPa, the monoclinic phase of Na−AlGe-NAT transforms into a tetragonal structure with the unit-cell composition of $Na_8Al_8Ge_{12}O_{40}\cdot 16H_2O$, revealing pressure-induced hydration and a unit cell volume contraction. Unlike in the Na−Al,Si-paranatrolite phase, however, the sodium cations in the Na−AlGe-NAT maintain a 6-fold coordination in the monoclinic structure and only become 7-fold coordinated at higher pressures in the tetragonal structure. When comparing the pressure-induced hydration in the observed natrolite-type zeolites, Na−AlGe-NAT appears to have a nonauxetic framework and reveals the highest onset pressure for complete superhydration.

Introduction

Zeolites, a representative family of microporous materials, are a well-defined class of crystalline framework materials.[1] They have three-dimensional structures arising from a corner-linked framework of $[TO_4]$ coordination polyhedra (T = Si, Al, Ge, Ga, and so forth). The frameworks generally are very open and contain channels and cavities where charge-balancing cations are located together with absorbed water molecules. The cations often have a high degree of mobility, and the water molecules are readily lost and reabsorbed. At present, some 190 naturally occurring and synthetic zeolite species have been reported in the literature with the opening sizes to the pores and channels ranging from 0.2 to 2 nm.[2] Each structural and chemical feature of a zeolite contributes to the unique catalytic, molecular sieving, and selective ion-exchange properties. In addition, the flexible linkages between tetrahedra and within the secondary building units allow the structural and chemical tuning of a given zeolite as a function of composition, temperature, and pressure.[3−5]

Recent interests in the high-pressure chemistry of zeolites stem from the discovery of pressure-induced hydration (PIH) and auxetic framework behavior in aluminosilicate natrolite and its synthetic gallosilicate analogues.[6−10] The natrolite framework is composed of T_5O_{10} (T = Si, Al, Ge, Ga, and so forth) tetrahedral units that are connected along the *c*-axis forming the so-called natrolite chains.[11] This mode of linkage between the chains creates helical 8-ring channels along the *c*-axis with $T_{10}O_{20}$ windows intersecting perpendicular to the channel. At ambient conditions, the aluminosilicate natrolite has an ordered distribution of Al and Si over the T-sites with *Fdd*2 (orthorhombic) symmetry and sodium cations located along the channels and water molecules close to the $T_{10}O_{20}$ windows.[12,13] When subjected to hydrostatic pressure mediated by a water-containing pressure medium, the aluminosilicate natrolite ($Na_{16}Al_{16}Si_{24}O_{80}\cdot 16H_2O$) shows an abrupt volume expansion of ca. 7% near 1 GPa, followed by a contraction of ca. 4% above 1.2 GPa.[7] This anomalous behavior is due to the successive uptake of water molecules from the pressure-transmitting media facilitated by the auxetic properties of the natrolite framework,[14] which gives rise to an ordered-paranatrolite ($Na_{16}Al_{16}Si_{24}O_{80}\cdot 24H_2O$) and a superhydrated-natrolite ($Na_{16}Al_{16}Si_{24}O_{80}\cdot 32H_2O$) phases, respectively. The ordered-paranatrolite (and natural paranatrolite) phase with

* Corresponding author. E-mail: tvogt@mailbox.sc.edu.
[†] Yonsei University.
[‡] Brookhaven National Laboratory.
[§] State University of New York.
[||] University of South Carolina.

10.1021/jp106964j
Published on Web 10/15/2010

an intermediate water content of 12 per 40 framework oxygen (O_f) is characterized by a monoclinic distortion of the unit cell, compared to the orthorhombic phases of both the original and the superhydrated natrolites, and the Na cations have unusual 7-fold coordination environments created by alternating two water bridges along the longer axis of the elliptical channels.[7] As a result, the density of the ordered-paranatrolite phase is lower than those of the original and the superhydrated phases. These intriguing structural changes leading to PIH and unit-cell volume expansion in natrolites thus demonstrate the unique role that hydrostatic pressure can play in controlling the geometry and chemistry of microporous materials.

The effect of the framework (and nonframework) cation substitution on superhydration has already been investigated in the gallosilicate analogues.[6,10] The onset pressure of superhydration has been reduced to ca. 0.6 GPa in a sodium gallosilicate natrolite, whereas the superhydrated state of a potassium counterpart was found to be recoverable upon pressure release.[10] Increased flexibility of the gallium substituted framework accounts for the onset of superhydration at a lower pressure. The compositional changes of the framework can be interpreted as chemical pressure leading to structural distortions as observed under hydrostatic pressures. Both Na−Al,Si-natrolite and Na−GaSi-NAT structures show PIH and a concomitant volume expansion indicating similar atomistic mechanisms at work. The rearrangement of the potassium cations in $K_{7.9(5)}Ga_8Si_{12}O_{40}\cdot 12.2(2)H_2O$ under pressure was suspected to play a crucial role in stabilizing the newly formed superhydrated water nanostructures inside the channels. Lowering the onset pressure is desirable in order to be able to use pressure-induced volume expansion to enhance cation exchange or catalytic activities. Irreversible superhydration has the potential to immobilize tritiated water (THO) or other pollutant atoms or molecules under pressure. Further control over the framework and nonframework composition has therefore been explored, and we report here on the high-pressure chemistry of a sodium aluminogermanate natrolite and compare its behavior to the Al,Si and Ga,Si analogues.

Experimental Section

High-Pressure Synchrotron X-ray Powder Diffraction. The synthesis of the sodium aluminogermanate natrolite (Na−AlGe-NAT) was described in detail by Tripathi et al.[15] Initial characterization and screening to find suitable experimental conditions were performed by using a symmetric diamond-anvil cell (DAC) and an imaging plate detector at 5A-HFMS beamline at Pohang Accelerator Laboratory (PAL). In situ high-pressure high-resolution synchrotron X-ray powder diffraction experiments were performed at the X14A beamline at the National Synchrotron Light Source (NSLS) at Brookhaven National Laboratory (BNL). The primary white beam from the bending magnet was monochromatized by using a Si (111) crystal, and sets of parallel slits were used to create a ~400 μm beam of monochromatic X-rays with a wavelength of 0.6833 Å. A Si-strip detector prototype consisting of a monolithic array of 640 silicon diodes coupled to a set of BNL's HERMES application-specific integrated circuits (D.P. Siddons, private communications) was used to collect high-resolution powder diffraction data ($\Delta d/d \approx 10^{-3}$). The Si-strip detector covered 3.2° in 2θ and was stepped in 2° intervals over the angular range of 3.5−35.5° with counting times of 30s per step. The wavelength of the incident beam was determined from a LaB6 standard (SRM 660).

As a reference, ambien- pressure data were measured by using a 0.5 mm diameter capillary filled with the ground sample of the Na−AlGe-NAT from the batch used for the previous single-crystal study.[15] A modified Merrill-Bassett DAC was used for the high-pressure experiments, equipped with two type-I diamond anvils (culet diameter of 800 μm) and slotted tungsten-carbide supports. A stainless-steel foil of 250 μm thickness was preindented to a thickness of about 100 μm, and a 500 μm hole was obtained by electro-spark erosion. The powdered sample of the Na−AlGe-NAT was placed in the gasket hole together with some ruby chips for in situ pressure measurements. A methanol:ethanol:water (16:3:1 by volume) mixture was used as hydrostatic pressure-transmitting medium in the DAC. The pressure the sample was exposed to in the DAC was measured by detecting the shift in the R1 emission line of the included ruby chips (precision: ±0.05 GPa).[16] The sample was equilibrated for about 10 min in the DAC at each measured pressure. After each powder diffraction pattern was collected, the pressure was increased in increments of ~0.5 GPa.

The structural refinements were performed by using the Rietveld method and the GSAS suite of programs.[17−19] The starting model for the refinement was taken from the previous single-crystal study.[15] It was soon realized, however, that the measured patterns between the ambient condition and 1.70 GPa deviate significantly for the tetragonal unit cell. Preliminary indexing of the ambient powder pattern suggested a monoclinic unit cell similar to the one observed for the Al,Si-paranatrolite phase.[7] An Al/Ge-disordered framework from the paranatrolite unit cell was then constructed and used as a starting model. The background was fitted by using a linear interpolation between selected positions in 2θ. The pseudo-Voigt profile function proposed by Thompson et al. was used to model the observed Bragg peaks.[20] In order to reduce the number of parameters, isotropic displacement factors were refined by grouping the framework oxygen atoms and the nonframework cations and water oxygen atoms. Geometrical soft-restraints on the T−O (T = Al, Ge) and O−O bond distances of the tetrahedra were applied: the T−O distances were restrained to a value of 1.750 ± 0.001 Å, and the O−O distances were restrained to a value of 2.858 ± 0.005 Å. Furthermore, a site disordered occupation of 40% Al and 60% Ge was fixed for the tetrahedral sites, following the previously established elemental-analysis results.[15] The sodium occupancy was also fixed to the total Al content on the basis of the previous single-crystal study.[15] The sites for water molecules, modeled by using only the oxygen scattering factor, showed nearly full occupancies and hence were fixed to be fully populated in later stages of the refinements. In the final stages of the refinements, convergence was achieved by refining simultaneously all profile parameters, scale factor, lattice constants, 2θ zero, and the atomic positional and thermal displacement parameters. The synchrotron X-ray powder diffraction pattern at each measured pressure is shown in Figure 1. The final refined parameters from the ambient and 2.27 GPa models are summarized in Tables 1 and 2, respectively, and the selected bond distances and angles are presented in Tables 3 and 4.

Results and Discussion

As outlined above, the crystal structure of in Na−AlGe-NAT at ambient pressure is found to be different from the one previously established in a single-crystal study.[15] The refined unit-cell formula of $Na_8Al_8Ge_{12}O_{40}\cdot 12H_2O$ indicates an increase in the water content by 50% compared to the $Na_8Al_8Ge_{12}O_{40}\cdot 8H_2O$ based on single-crystal data. This led to a monoclinic

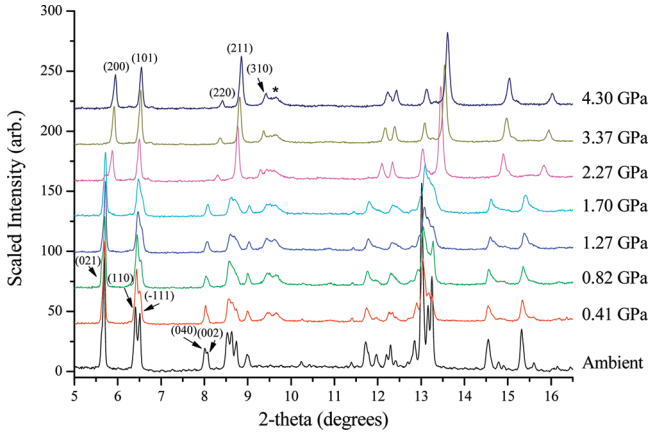

Figure 1. Synchrotron X-ray powder diffraction patterns measured of Na−AlGe-NAT as a function of pressure mediated by an alcohol and water mixture. Ambient data were measured by using dry powder packed in a 0.5 mm capillary. Miller indices are shown for the first several Bragg peaks. The asterisk mark indicates high-order harmonic background from gasket.

TABLE 1: Final Refined Atomic Coordinates for the Na−AlGe-NAT at Ambient Conditions[a]

atom	site	*x*	*y*	*z*	U_{iso}
T1	4*a*	0.5	0.3736(6)	0	0.021
T2	4*a*	0.2038(7)	0.3343(7)	0.2101(7)	0.021
T3	4*a*	0.5198(5)	0.0910(5)	0.3039(5)	0.021
T4	4*a*	0.9445(5)	0.4629(5)	0.0810(5)	0.021
T5	4*a*	0.3806(6)	0.2194(6)	0.4236(6)	0.021
O1	4*a*	0.532(4)	0.034(1)	0.437(1)	0.025
O2	4*a*	0.466(4)	0.046(1)	0.149(1)	0.025
O3	4*a*	0.375(4)	0.166(1)	0.286(1)	0.025
O4	4*a*	0.160(3)	0.192(1)	0.470(3)	0.025
O5	4*a*	0.332(4)	0.305(1)	0.375(1)	0.025
O6	4*a*	0.082(3)	0.276(1)	0.079(2)	0.025
O7	4*a*	0.399(2)	0.361(1)	0.139(1)	0.025
O8	4*a*	0.047(4)	0.405(1)	0.215(1)	0.025
O9	4*a*	0.786(1)	0.113(1)	0.353(1)	0.025
O10	4*a*	0.677(1)	0.442(1)	0.029(3)	0.025
Na1	4*a*	0.176(7)	0.156(3)	0.048(6)	0.040
Na2	4*a*	0.571(6)	0.112(4)	−0.045(4)	0.040
OW1	4*a*	0.163(9)	0.068(3)	−0.123(6)	0.040
OW2	4*a*	0.920(12)	0.071(4)	0.103(8)	0.040
OW3	4*a*	0.720(11)	0.224(4)	0.193(7)	0.040

[a] Space group C*c*, a = 6.7499(6) Å, b = 19.563(2) Å, c = 10.1816(9) Å, β=107.82(1)°, V = 1280.0(2) Å^3. In F*d* setting, a = 19.3920(5) Å, b = 19.5630(5) Å, c = 6.7499(2) Å, β=91.52(1)°, V = 2560(1) Å^3, $x' = z/2$, $y' = y$, $z' = -x + z/2$. $_wR_p$ = 0.074, R_p = 0.055. Esd's are in parentheses. Each T site contains Al/Ge in 0.4/0.6 fraction. Soft constraints were used for framework interatomic distances. Isotropic displacement parameters, U_{iso} (Å^2), were restrained to be the same for the T-site atoms, framework oxygen atoms, and nonframework species (esds' are in the range of 0.001 and 0.002). All sites are fully occupied.

distortion and expansion of the unit-cell volume by ca. 6% (Figure 2). $Na_8Al_8Ge_{12}O_{40}\cdot 8H_2O$ is highly sensitive to humidity, and the ground sample has a larger exposed surface area and therefore readily takes up water. In fact, this is analogous to what is observed in the Na−Al,Si-natrolite-to-Na−Al,Si-paranatrolite transformation where the paranatrolite phase with the same monoclinic symmetry as in the Al,Ge phase has 12 H_2O per 40 framework oxygen (O_f), exists only in a wet environment, and readily loses water upon excavation to convert back to a natrolite phase with orthorhombic symmetry and 8 H_2O per 40 O_f.[21,22] Compared to the Na−Al,Si-natrolite phase, the unit-cell volume of the monoclinic Na−AlGe-NAT phase at ambient conditions is ca. 14% larger (Figure 2). On the other hand, the unit-cell volume of the orthorhombic Na−AlGe-NAT, that is, the single-crystal model with 8 H_2O per 40 O_f, happens to be similar to that of the natural paranatrolite in wet conditions.

TABLE 2: Final Refined Atomic Coordinates for the Na−AlGe-NAT at 2.27 GPa[a]

atom	site	*x*	*y*	*z*	U_{iso}
T1	4*a*	0	0	0	0.030
T2	16*e*	0.9425(1)	0.1340(1)	0.6202(1)	0.030
O1	8*d*	0.6195(2)	0.25	0.125	0.030
O2	16*e*	0.0379(1)	0.1417(1)	0.4422(1)	0.030
O3	16*e*	−0.0085(3)	0.1083(1)	0.8549(3)	0.030
Na1	8*d*	0.296(2)	0.25	0.125	0.036
OW1	8*d*	−0.151(2)	0.25	0.125	0.036
OW2	8*d*	0.101(2)	0.25	0.125	0.036

[a] Space group I-42*d*, a = 13.3182(9) Å, c = 6.7433(7) Å, V = 1196.1(2) Å^3. $_wR_p$ = 0.075, R_p = 0.045. Esd's are in parentheses. Each T site contains Al/Ge in 0.4/0.6 fraction. Soft constraints were used for framework interatomic distances. Isotropic displacement parameters, U_{iso} (Å^2), were restrained to be the same for the framework atoms and nonframework species (esds' are in the range of 0.001 and 0.002). All sites are fully occupied.

The structure of the monoclinic Na−AlGe-NAT phase is, however, different from the one of the Na−Al,Si-paranatrolite phase. Unlike the paranatrolite where Al and Si atoms occupy two and three distinct framework T-sites, respectively, the framework of the Na−AlGe-NAT is characterized by a complete disordering of the Al and Ge atoms over the five T-sites with a 2:3 ratio (Table 1). There are also some significant differences in the distribution of the nonframework sodium cations and water molecules in the monoclinic Na−AlGe-NAT and the Na−Al,Si-paranatrolite. In both models, two sodium sites are located along the center of the helical 8-ring channels, and three water sites are found near the sodium sites close to the channel walls. The newly located water molecule OW3 in the monoclinic Na−AlGe-NAT, however, bonds only to three framework oxygens and not to the central sodium cation (Figure 3). As a result, the central sodium cations all remain six-coordinated by four framework oxygen atoms and two water molecules with distances in the range between 2.39(6) Å and 2.89(7) Å (Table 3). In the Na−Al,Si-paranatrolite phase, all the water molecules bridge the central sodium cations to create a 7-fold coordination.[7] When applying hydrostatic pressure, the unit cell of the monoclinic Na−AlGe-NAT gradually contracts up to ca. 2 GPa, and the bulk modulus B_0 is fitted to 72(3) GPa with its pressure derivative fixed at 4 (Figure 2).[23]

Further increase in pressure above 2 GPa leads to an abrupt volume contraction of the unit cell of the Na−AlGe-NAT structure by ca. 4.6% (Figure 2). Concomitant to this, the monoclinic Na−AlGe-NAT 12H_2O phase transforms to a phase with a tetragonal structure. Rietveld refinement obtained by using data measured at 2.27(5)GPa shows that the water content has increased by 30% compared to the monoclinic unit cell to $Na_8Al_8Ge_{12}O_{40}\cdot 16H_2O$ (Tables 1 and 2). This behavior is in marked contrast to what is observed in both Na−Al,Si-natrolite and Na-GaSi-NAT where the PIH is accompanied by a volume expansion because of the significant increase in the *a* and *b* lattice parameters of the orthorhombic unit cell (see Figure 1 in ref 6). However, in both the monoclinic-to-tetragonal-Na−AlGe-NAT and the Na−Al,Si-paranatrolite-to-superhydrated-Na−Al,Si-natrolite transitions, a volume contraction occurs, and a phase with 12 H_2O per 40 O_f transforms to one with 16 H_2O per 40 O_f.[7] The distribution of the nonframework cations and water molecules in the tetragonal Na−AlGe-NAT

TABLE 3: Selected Interatomic Distances (Angstroms) and Angles (Deg) for the Na−AlGe-NAT at Ambient Conditions[a]

T1−O4	1.764(5)	T2−O5	1.736(5)	T3−O1	1.746(5)
T1−O7	1.759(4)	T2−O6	1.750(5)	T3−O2	1.748(5)
T1−O9	1.753(5)	T2−O7	1.773(4)	T3−O3	1.737(5)
T1−O10	1.762(5)	T2−O8	1.745(5)	T3−O9	1.764(5)
av. T1−O	1.760(2)	av. T2−O	1.751(2)	av. T3−O	1.749(3)
T4−O1	1.739(5)	T5−O3	1.739(5)	T3−O1−T4	132.9(7)
T4−O2	1.750(5)	T5−O4	1.776(5)	T3−O2−T4	142.7(11)
T4−O8	1.747(5)	T5−O5	1.743(5)	T3−O3−T5	123.5(9)
T4−O10	1.766(5)	T5−O6	1.747(5)	T1−O4−T5	150.8(11)
av. T4−O	1.751(3)	av. T5−O	1.751(3)	T2−O5−T5	126.1(6)
Na1−O2	2.87(6)	Na2−O1	2.87(7)	T2−O6−T5	135.5(10)
Na1−O3	2.39(6)	Na2−O2	2.64(5)	T1−O7−T2	152.7(8)
Na1−O5	2.57(6)	Na2−O5	2.70(6)	T2−O8−T4	126.4(7)
Na1−O6	2.49(6)	Na2−O8	2.43(5)	T1−O9−T3	141.3(8)
Na1−OW1	2.43(7)	Na2−OW1	2.76(6)	T1−O10−T4	143.4(11)
Na1−OW2	2.57(7)	Na2−OW2	2.51(9)		
OW1−O2	2.93(7)	OW1−O10	2.89(7)	OW3−O4	2.73(9)
OW1−O7	2.89(7)	OW3−O3	3.00(8)	OW3−O9	2.67(9)

[a] Estimated standard deviations are in parentheses. Standard deviations are computed by using $\sigma = (1)/(n)(\sum_{i=1}^{n} \sigma_i^2)^{1/2}$.

TABLE 4: Selected Interatomic Distances (Angstroms) and Angles (Deg) for the Na−AlGe-NAT at 2.27 GPa[a]

T1−O3	1.747(1) × 4	Na1−O1	2.50(1) × 2
T2−O1	1.751(1)	Na1−O2	2.92(2) × 2
T2−O2	1.751(1)	Na1−OW1	2.23(2) × 2
T2−O2	1.753(1)	Na1−OW2	2.60(3)
T2−O3	1.746(1)	OW1−OW2	2.93(2) × 2
av. T2−O	1.750(1)	OW2−O2	2.71(1) × 2
T2−O1−T2	123.8(2)	OW2−O3	3.00(1) × 2
T2−O2−T2	131.1(1)		
T1−O3−T2	134.0(1)		

[a] Estimated standard deviations are in parentheses. Standard deviations are computed by using $\sigma = (1)/(n)(\sum_{i=1}^{n} \sigma_i^2)^{1/2}$.

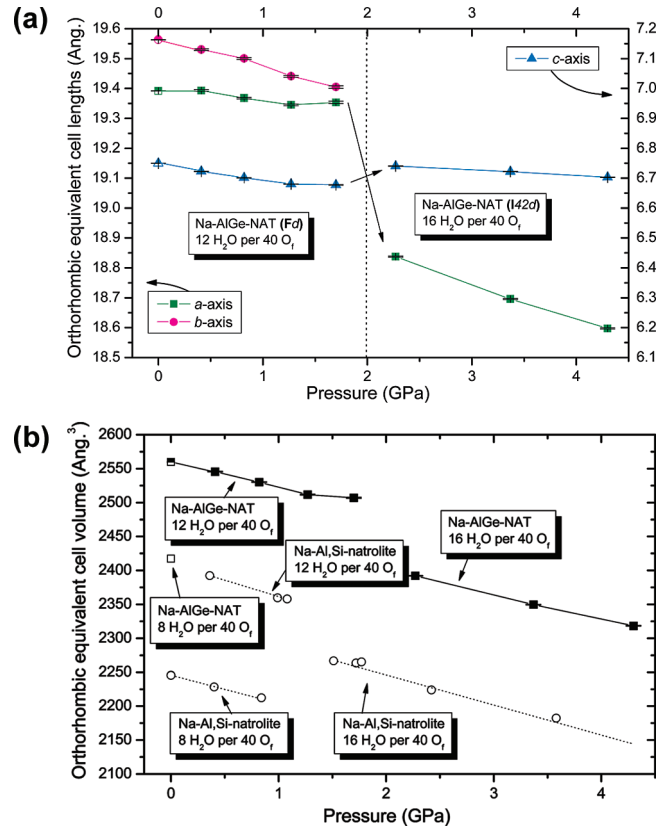

Figure 2. (a) Changes in the unit-cell edge lengths (angstroms) and (b) volume of the Na−AlGe-NAT as a function of hydrostatic pressure. The values were normalized to an F*dd*2 equivalent setting for comparison. Half-filled symbols represent data taken at ambient conditions. The open square represents the unit-cell volume of the Na−AlGe-NAT measured from the previous single-crystal study. The pressure-induced changes of the unit cell volume of Na−Al,Si-natrolite is shown by using open circles for comparison. The overlap of the phase regions for Na−Al,Si-natrolite below 1 GPa is a result of hysteresis upon pressure release. For more details, see ref by Lee et al.[7] Estimated standard deviations (esd's) are smaller than the individual symbols.

is very similar to that of the superhydrated aluminosilicate natrolite (Figure 3). The central sodium cations are now 7-fold coordinated by four framework oxygen atoms and three water molecules (Table 4). The OW1 water bridges the neighboring sodium cations with an interatomic distance of 2.23(2) Å, whereas the OW2 water bonds to one sodium cation at 2.60(3) Å and four framework oxygen atoms in the range between 2.71(1) and 3.00(1) Å (Figure 3 and Table 4). The two water sites are separated by 2.93(2) Å, which is comparable to what is found in the superhydrated aluminosilicate natrolite with two water separation distances of 2.80(4) Å and 3.09(4) Å.[9] As such, a hydrogen-bonded helical water chain can be envisaged to form around the central sodium cations along the elliptical channel of the superhydrated tetragonal Na−AlGe-NAT. The derived bulk modulus of 61(1) GPa of the superhydrated tetragonal Na−AlGe-NAT is marginally smaller than the monoclinic phase below 2 GPa (Figure 2).

The atomistic mechanisms of PIH deduced from crystallographic studies of Al,Si and Ga,Si natrolites can be understood by a rotating-squares model[24] based on rigid tetrahedral units and soft hinges resulting in a pore and volume expansion and concomitant PIH (superhydration). This mechanism has been independently discussed in the literature as one of the ways that auxetic behavior of materials manifests itself at the atomistic scale.[25] Auxetic materials are materials with negative Poisson's ratios that lead to a thinning of material when compressed or fattening when stretched in a perpendicular direction.[26,27] Recently, Grima et al showed experimentally that the aluminosilicate natrolite is indeed an auxetic zeolite with negative Poisson ratios.[28] The rotation angle Ψ of the fibrous chain, which is the mean of the angles between the sides of the quadrilateral around the T_5O_{10} tetrahedral building unit (T = Si, Al, Ge, Ga, and so forth) projected on to the plane perpendicular to the channel,[4] relates to the opening of the channel because the larger Ψ, the more elliptical the channel opening will be (Figure 4). Water uptake in natrolites is related to the size and ellipticity of the channel openings.[29,30] The expansion of the *a* and *b* lattice

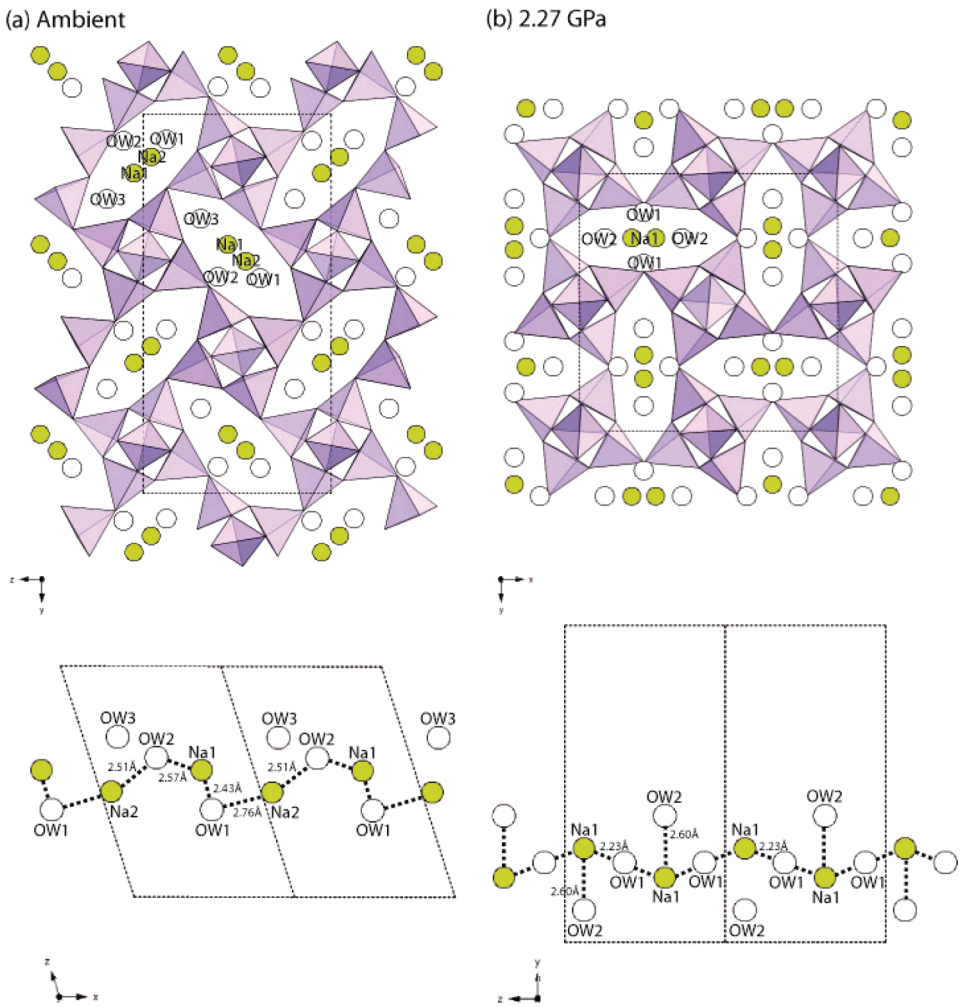

Figure 3. Polyhedral representations of the Na−AlGe-NAT (a) at ambient conditions and (b) at 2.27 GPa, viewed along the chain/channel axis. Filled circles represent sodium cations; open circles represent water oxygen atoms. Filled tetrahedra illustrate disordered distribution of Al/Ge atoms in the framework T-sites. Dotted lines define a unit cell. Expanded views of the distribution of the nonframework sodium cations and water molecules are shown perpendicular to the channel axes under the respective models.

parameters observed in the GaSi- and AlSi-NAT systems during PIH are the result of a coordinated rotation of T_5O_{10} subunits. In both PIH and pressure-induced insertion of argon into the Na−Al,Si-natrolite $8H_2O$ structure, the chain rotation angle is at a minimum in the Na−Al,Si-paranatrolite phase near 20.5° and then increases because of superhydration abruptly to above 23.7° and subsequently to near 26° at 5 GPa.[7,14] In the case of the monoclinic $Na_8Al_8Ge_{12}O_{40}\cdot 12H_2O$, we observe a slight increase of Ψ by about 0.5° as the pressure increases up to near 2 GPa (Figure 4a). Then, we observe a more pronounced increase of the chain rotation angle Ψ after 2 GPa to near 25.5°, reminiscent of the increase observed during the transition from the parantrolite $Na_8Al_8Si_{12}O_{40}\cdot 12H_2O$ to the superhydrated $Na_8Al_8Si_{12}O_{40}\cdot 16H_2O$ phase. The substitution of the larger Ge for Si leads to a reduction of the chain rotation angle in the monoclinic phase to near 23°, whereas the ambient phases of $Na_8Al_8Si_{12}O_{40}\cdot 8H_2O$ and $Na_8Ga_8Si_{12}O_{40}\cdot 8H_2O$ both have chain rotation angles between 25 and 26°. In our investigations of the Na−GaSi-NAT system,[6] we observed a behavior similar to that of the Na−Al,Si-NAT system, and the GaSi framework responds to superhydration by decreasing the chain rotational angle by about 1° and increasing its unit cell volume by about 1.5% during PIH near 0.6 GPa. Subsequently, in its $Na_8Ga_8Si_{12}O_{40}\cdot 16H_2O$ superhydrated state near 3 GPa, the chain rotation angle returns to a value close to the one it has at ambient conditions (∼26°). There are no indications of a paranatrolite-type phase with 12 H_2O per 40 O_f in the Na−GaSi-NAT system. A comparison of the bulk moduli of the superhydrated phases and the PIH-onset pressures in Na−Al,Si-NAT (43(2) GPa and ∼1 GPa), Na−GaSi-NAT (52(2) GPa and ∼0.6 GPa), and Na−AlGe-NAT (61(1) GPa and ∼2 GPa) indicates that the latter has the stiffest framework in the superhydrated state and requires the highest onset pressure to transform into this state. Furthermore, the fact that in Na−AlGe-NAT no initial reduction of the chain rotation angle and no unit-cell expansion during PIH is observed is in marked contrast to both the Na−Al,Si-NAT and the Na-GaSi-NAT systems. Smaller chain rotation angles translate into less elliptical channel openings facilitating water uptake (see Figure 4a,b). $Na_8Ga_8Si_{12}O_{40}\cdot 8H_2O$ has the largest Ψ and the most elliptical channel openings. The ellipticity of its helical eight-ring window slightly decreases whereas its size increases before PIH takes place near 0.6 GPa. $Na_8Al_8Si_{12}O_{40}\cdot 8H_2O$ has a Ψ ca. 1° smaller at ambient conditions than that of the $Na_8Ga_8Si_{12}O_{40}\cdot 12H_2O$. An initial increase of the chain rotation angle increases the ellipticity but reduces the size of the channel openings before PIH. The smallest Ψ observed at ambient conditions in the monoclinic $Na_8Al_8Ge_{12}O_{40}\cdot 12H_2O$ phase near 23° appears to be below a threshold level where the channel opening already allows for a partial hydration and subsequently for an additional 50% uptake to transform

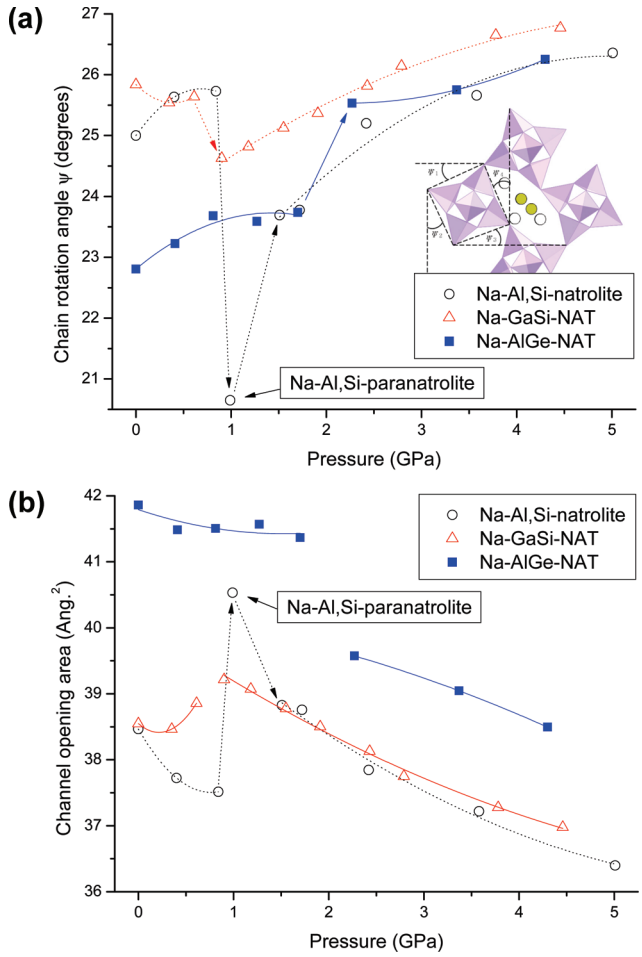

Figure 4. Pressure dependence of the (a) average chain rotation angle Ψ and (b) channel opening (Å^2) of the Na−AlGe-NAT, compared to those from Na−Al,Si-natrolite and Na−GaSi-NAT. The inset figure illustrates the chain rotation angles of Na−AlGe-NAT in a monoclinic phase.

Na−AlGe-NAT 8H_2O to Na−AlGe-NAT 12H_2O. During the PIH from $Na_8Al_8Ge_{12}O_{40}\cdot 12H_2O$ to $Na_8Al_8Ge_{12}O_{40}\cdot 16H_2O$, a unit-cell contraction is observed. In the Na−Al,Si-NAT system, a unit-cell contraction is also observed during the transition from the $Na_8Al_8Si_{12}O_{40}\cdot 12H_2O$ to superhydrated $Na_8Al_8Si_{12}O_{40}\cdot 16H_2O$ phase (see Figure 2b). After both transitions, the chain rotation angles Ψ subsequently increases the ellipticity and reduces the size of the channel openings under pressure. At pressures above 4 GPa, the chain rotation angles and water contents in the superhydrated phases (16 H_2O per 40 O_f) of the AlSi, AlGe, and GaSi analogues are essentially the same. Although the size of the channel openings in the Na−AlSi-NAT and Na−GaSi-NAT systems in the superhydrated state are essentially the same, the Na−AlGe-NAT channel opening remains ca. 1 Å^2 larger.

The different behavior of the AlSi, AlGe, and GaSi natrolite phases under pressure points to a complex interplay between chemical and hydrostatic pressure: in the Na−AlGe-NAT system, where the disordered framework T-sites are occupied by 40% Al and 60% Ge, the chemical pressure created by the larger average T cation size results in the smallest chain rotation angle Ψ and the largest channel openings (~42 Å^2) at ambient conditions, which facilitates the uptake of water. The result is a hydration of $Na_8Al_8Ge_{12}O_{40}\cdot 8H_2O$ to $Na_8Al_8Ge_{12}O_{40}\cdot 12H_2O$. This initial hydration leads to a phase which resembles the $Na_8Al_8Si_{12}O_{40}\cdot 12H_2O$ parantrolite phase. In both the Na−Al,Si-natrolite and the Na-GaSi-NAT at ambient conditions, the smaller average cation sizes result in larger chain rotation angles Ψ which are changed under pressure to facilitate hydration. In the case of the Na−GaSi-NAT phase, it appears that a reduction of Ψ by about 1.5° permits superhydration at 0.6 GPa. This occurs because of the auxetic properties of the GaSi framework, where a lattice expansion under pressure in the *ab*-plane creates the ellipticity and size required for water uptake. In the case of the ambient Na−Al,Si-natrolite phase with the smallest average T cation size, an initial 50% superhydration under pressure creates a $Na_8Al_8Si_{12}O_{40}\cdot 12H_2O$ parantrolite phase which has a very narrow phase width under pressure and then transforms into a superhydrated $Na_8Al_8Si_{12}O_{40}\cdot 16H_2O$. Both PIHs in the Na−Al,Si-NAT system can be understood as the result of the auxetic properties of the AlSi framework, where a volume expansion due to correlated rotations of T_5O_{10} units leads to a smaller chain rotation angle Ψ allowing water to enter the framework. A way to rationalize the observed pressure behavior in the Na−AlGe-NAT system is that the increase of the average size of the T cations within the T_5O_{10} units has created a chemical pressure that has produced a favorable channel-opening geometry to allow water absorption at ambient conditions and transform the $Na_8Al_8Ge_{12}O_{40}\cdot 8H_2O$ phase to a $Na_8Al_8Ge_{12}O_{40}\cdot 12H_2O$ phase. This phase, which resembles the $Na_8Al_8Si_{12}O_{40}\cdot 12H_2O$ parantrolite phase, has a larger phase width as a function of pressure and is subsequently superhydrated into a $Na_8Al_8Ge_{12}O_{40}\cdot 16H_2O$ phase above 2 GPa.

Conclusion

In summary, we have structurally characterized a new stable form of Na−AlGe-NAT at ambient conditions. In view of the same monoclinic symmetry and water content of 12 H_2O per 40 O_f as observed in the Al,Si-paranatrolite phase, we rationalize this phase as an analogue of the Na−Al,Si-parantrolite phase. However, there are differences in the distribution of the nonframework sodium cations and water molecules in the aluminosilicate paranatrolite and the aluminogermanate natrolite. Furthermore, in contrast to the Na−Al,Si-parantrolite phase, the monoclinic Na−AlGe-NAT is stable over a wide pressure range up to ca. 2 GPa where it then transforms into a tetragonal phase with a smaller unit-cell volume by PIH and further increases its water content to now 16 H_2O per 40 O_f. In this tetragonal Na−AlGe-NAT phase above 2 GPa, the coordination number of the sodium cation increases to seven by the formation of a hydrogen-bonded helical water chain. The high-pressure tetragonal AlGe phase is more compressible than its low-pressure monoclinic paranatrolite-related phase. The comparison of the Na−Al,Si-natrolite, Na−GaSi-NAT, and Na−AlGe-NAT systems which have a common framework topology that can display auxetic behavior under pressure reveals a complex interplay between hydrostatic and chemical pressure resulting in very distinct behaviors up to pressures near 2 GPa. We hope that our work on the intricate high-pressure crystallography and PIH of chemical analogues with natrolite structures can be followed up by modeling and simulation studies which might shed more light on the detailed atomistic mechanisms. Pressure-induced insertion of other molecules such as CO_2, CH_4, and H_2 are highly topical and could benefit from a more detailed understanding and predictability.

Acknowledgment. This work was supported by the Global Research Lab Program of the Ministry of Education, Science and Technology (MEST) of the Korean Government. The authors thank Dr. Hyun-Hwi Lee for the operation of the 5A-

HFMS beamline. D.H.S. thanks the support from the BK21 program to the Institute of Earth, Atmosphere, and Astronomy at Yonsei University. Experiments at PAL were supported in part by the Ministry of Science and Technology (MOST) of the Korean Government and Pohang University of Science and Technology (POSTECH). Research carried out in part at the NSLS at BNL is supported by the U.S. Department of Energy, Office of Basic Energy Sciences.

Supporting Information Available: A full list of final refined atomic coordinates for the Na−AlGe-NAT at all measured pressures. This material is available free of charge via the Internet at http://pubs.acs.org.

References and Notes

(1) Breck, D. W. *Zeolite Molecular Sieves*; Krieger: Malabar, FL, 1984.
(2) Baerlocher, C.; McCusker, L. B.; Olson, D. H. *Atlas of Zeolite Framework Types*, 6th ed.; Elsevier: Amsterdam, 2007.
(3) Baur, W. H.; Joswig, W. *N. Jb. Miner. Mh.* **1996**, *171*.
(4) Baur, W. H.; Kassner, D.; Kim, C.-H.; Sieber, N. H. *Eur. J. Mineral.* **1990**, *2*, 761.
(5) Belitsky, I. A.; Fursenko, B. A.; Gubada, S. P.; Kholdeev, O. V.; Seryotkin, Y. V. *Phys. Chem. Minerals* **1992**, *18*, 497.
(6) Lee, Y.; Hriljac, J. A.; Kim, S.-J.; Hanson, J. C.; Vogt, T. *J. Am. Chem. Soc.* **2003**, *125*, 6036.
(7) Lee, Y.; Hriljac, J. A.; Parise, J. B.; Vogt, T. *Am. Mineral.* **2005**, *90*, 252.
(8) Lee, Y.; Martin, C. D.; Parise, J. B.; Hriljac, J. A.; Vogt, T. *Nano Lett.* **2004**, *4*, 619.
(9) Lee, Y.; Vogt, T.; Hriljac, J. A.; Parise, J. B.; Artioli, G. *J. Am. Chem. Soc.* **2002**, *124*, 5466.
(10) Lee, Y.; Vogt, T.; Hriljac, J. A.; Parise, J. B.; Hanson, J. C.; Kim, S. J. *Nature* **2002**, *420*, 485.
(11) Pauling, L. *Proc. Nat. Acad. Sci.* **1930**, *16*, 453.
(12) Meier, W. M. *Z. Kristallogr.* **1960**, *113*, 430.
(13) Artioli, G.; Smith, J. V.; Kvick, A. *Acta Crystallogr.* **1984**, *C40*, 1658.
(14) Lee, Y.; Hriljac, J. A.; Vogt, T. *J. Phys. Chem. C* **2010**, *114*, 6922.
(15) Tripathi, A.; Johnson, G. M.; Kim, S.-J.; Parise, J. B. *J. Mater. Chem.* **2000**, *10*, 451.
(16) Bell, P. M.; Mao, H. K. Absolute pressure measurements and their comparison with the ruby fluorescence (R1) pressure scale to 1.5 Mbar. *Carnegie Inst. Washington Year Book* **1979**, *78*, 665.
(17) Larson, A. C.; VonDreele, R. B. *GSAS; General Structure Analysis System," Report LAUR 86−748*;, Los Alamos National Laboratory: Los Alamos, NM, 1986.
(18) Rietveld, H. M. *J. Appl. Crystallogr.* **1969**, *2*, 65.
(19) Toby, B. H. *J. Appl. Crystallogr.* **2001**, *34*, 210.
(20) Thompson, P.; Cox, D. E.; Hastings, J. B. *J. Appl. Crystallogr.* **1987**, *20*, 79.
(21) Chao, G. Y. *Can. Mineral.* **1980**, *18*, 85.
(22) Evans, H. T.; Konnert, J. A.; Ross, M. *Am. Mineral.* **2000**, *85*, 1808.
(23) Hazen, R. M.; Finger, L. W. *Comparative Crystal Chemistry*; John Wiley & Sons: New York, 1982.
(24) Grima, N. J.; Farrugia, P. S.; Caruana, C.; Gatt, R.; Attard, D. *J. Mater. Sci.* **2008**, *43*, 5962.
(25) Grima, J. N.; Jackson, R.; Alderson, A.; Evans, K. E. *Adv. Mater.* **2000**, *12*, 1912.
(26) Love, A. E. H. *A Treatise on the Mathematical Theory of Elsaticity*, 4th ed.; Dover: New York, 1944.
(27) Evans, K. E.; Nkansah, M. A.; Hutchinson, I. J.; Rogers, S. C. *Nature* **1991**, *353*, 124.
(28) Grima, J. N.; Gatt, R.; Zammit, V.; Williams, J. J.; Evans, K. E.; Alderson, A.; Walton, R. I. *J. Appl. Phys.* **2007**, *101*, 86102.
(29) Gatta, G. D. *Eur. J. Mineral.* **2005**, *17*, 411.
(30) Gatta, G. D. *Z. Kristallogr.* **2008**, *223*, 160.

JP106964J